Time-domain surface scan method

Article · May 2012

DOI: 10.1109/APEMC.2012.6237977

5 authors, including:

Mart Coenen
EMCMCC, Breda, the Netherlands
21 PUBLICATIONS **184** CITATIONS

SEE PROFILE

Time-Domain Surface Scan Method

Mart Coenen, Tom Gierstberg
EMCMCC
Eindhoven, the Netherlands
mart.coenen@emcmcc.nl
tom.gierstberg@emcmcc.nl

Arthur van Roermund, Anton de Koning, Teis Coenen
Eindhoven University of Technology
Eindhoven, the Netherlands
a.h.m.v.roermund@tue.nl
a.p.d.koning@student.tue.nl
t.j.coenen@tue.nl

***Abstract*— The necessity of using dedicated EMI-receivers and compliant spectrum analyzers with CISPR detectors is based on an outdated approach. The levels that people perceive from AM/FM radio reception and analogue modulated television broadcast signals as interference is taken as reference. In the meanwhile new detectors: C_AV and C_RMS have been defined of which the software algorithm is patented which, as such, is delaying the acceptance of these new detectors to be included in IEC CISPR 16-1-1. For most of the EMC related issues, there is little need for such specific detectors as one has to recalculate the nuisance that the total disturbing signal provokes per system bandwidth anyhow. The effect that an RF disturbance might have on a broadcasted RF signal with limited bandwidth will be completely different from e.g. sensor applications where broadband demodulation might occurs. As such, EMC compliant products may still cause nuisance when other detection criteria apply.**

Time-domain based EMC measurement systems have been developed with just a single RF input [1]. However, for most of the surface and 3D scanning applications 3 or 4 RF inputs are needed e.g. for measuring the 3 orthogonal E/H-field components and the other input is used for synchronisation. For such applications, modern 4-channel digital oscilloscopes can be used which have add-on mathematical analysis capabilities for the signals obtained. By taking time-domain data with sufficient sampling resolution, the influence onto other susceptible systems can be post-calculated by applying the complex response characteristic of the system being interfered. However efficient data reduction is a prerequisite to limit data storage and enable post-processing.

I. Introduction

The definition of EMC compliant EMI receivers and spectrum analysers with only a single RF input has blocked the development of real-time E/H-field scanning systems. These 'EMC' compliant receivers only deliver a single scalar amplitude value per frequency over a predefined bandwidth, weighted in a predetermined way by some detector response: Peak, Quasi-Peak, Average, RMS, C_AV, C_RMS, etc.

Measuring orthogonal E/H-fields is possible by using broadband sensors which measure RF power but which have (intentionally) no frequency selectivity. As such, only the dominant E/H-field component, Peak, RMS or Average weighted can be measured in a surface scan. The 3 orthogonal field amplitudes can be obtained successively but spectral information is lost.

To be able to reconstruct the far-field from near-field measurements it is necessary to have all orthogonal E/H-field amplitudes and their phases per frequency to represent the total complex field. Moreover, to calculate the interaction between (sub-)systems, the surface field distributions are of importance, both for radiation and irradiation. To calculate the influence of the measured signals onto another system, the propagation of these surface scanned fields have to be projected onto the surface scanned field sensitivity data of the target. Then the signals of interest have to be integrated over the bandwidth at which the target is sensitive. This bandwidth may extend from the functional bandwidth to e.g. the side-bands at which the sample/hold circuit oversamples the intended signal (and all harmonics and sidebands thereof).

II. Measurement System

The measurement system built comprises a 4-channel digital oscilloscope, if necessary to extend the frequency range, a 4-channel RF-mixer front-end, orthogonal E/H-field sensor probes and an X/Y/Z scanning table. In the chapter following, this will be further explained.

Figure 1 - Example of the digital scope used

For the 4-channel digital oscilloscope, an off-the-shelf LeCroy scope is used. This scope formally has 2 GHz analogue bandwidth per channel (where a -3 dB sensitivity bandwidth of 2,5 GHz was measured) and can sample with 5 or 10 Gs/s per channel. This scope, compared to other digital scopes available, has the advantage of having a direct MatLab® X-Stream data interface layer, which makes data transfer much faster and more efficient. With a memory depth of ≥ 10 Ms/channel, detailed information can be gathered and processed with a vertical resolution of 8 bits. Then, by means of over-sampling, the dynamic range is extended by $\sqrt{n}$, where

n is the over-sampling ratio but then limited in its repetitiveness by the maximum record length available.

By means of 4 external (close to) equal RF-mixers, driven by a 1-to-4 port RF-splitter, the RF-mixers are synchronously driven by a stable external local oscillator. In front of these RF-mixers band-pass filters are used of which the pass-band can be selected by a coaxial switch matrix, similar as defined in [1]. Following the RF-mixer's outputs, low-pass filters are used to suppress the upper sideband (and their harmonics). With the components chosen, the upper frequency of the oscilloscope can be extended to 20 GHz, all with 2 GHz bandwidth intervals. The phase and amplitude deviations per channel conversion path can be corrected for by providing a single RF signal, through an additional 1-to-4 port RF-splitter, to all 4 RF inputs in parallel. Skew, phase and amplitude deviations can be derived, as a function of frequency, for which the raw data obtained can be corrected for mathematically.

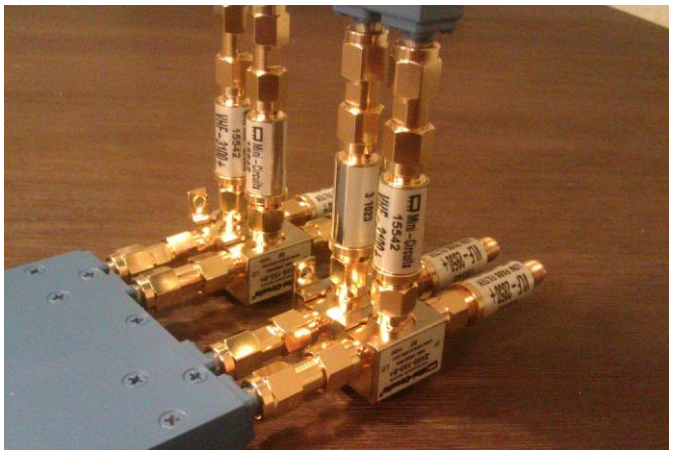

Figure 2 - 4 channel RF-mixer with 1:4 port divider, HP and LP filters

With the initial surface scanning experiments different commercially available H-field sensing probes were used to measure each single H-field component at a certain distance from the surface sequentially. There, the issue occurred that the spatial orientation of the center of the sensing probes, when putting it into its orthogonal orientations, gave too much overlay errors to enable a total field reconstruction. Also the probe correction data provided was found unreliable as no matching could be obtained with calculations.

Figure 3 - Photo of the orthogonal 3 axis H-field probe

An alternative H-field probe was developed with all three H-field sensing antennae orthogonal, see figure 3. The three orthogonal H-field sensing rod antennae are rotated over 45 degrees such that each field sensing element has the same distance towards the (flat) surface underneath. Each of these antennae is connected to a 50 Ω semi-rigid coaxial cable. Through the center of the H-field sensors an additional conductor is applied to enable the measurement of the E_z-field component. For the calibration of the H-field sensors a compact Helmholtz coil, diameter = 30 mm, was made which can be used up to 500 MHz. The transfer functions of the H-field sensing rod antennae are obtained by placing the probe in three orthogonal positions w.r.t. the normal of the flux in the center of the Helmholtz coils. A 3 x 3 transfer function matrix need to be obtained.

As a result of the orientation of these three rod antennae, the Cartesian H-field components have to be calculated by addition and substraction of the signals obtained. This can be done on the fly while doing the measurements or by using a look-up table and interpolation. Aside the orientation issue, also the H-field antenna conversion factors have to be taken into account (in worse case different for all 3 rod antennae). These corrections can easily be done in the frequency domain. The amplitude and skew corrected input signals have to be transferred to the frequency domain (using FFT), after which the frequency dependent corrections can be applied. Then the Cartesian axis correction needs to be carried out. The resulting signal can either be observed in the frequency domain e.g. as H-field amplitude/√Hz or in the time-domain after performing an IFFT over a predetermined bandwidth.

Figure 4 - X/Y/Z controlled measurement table

For the field scanning above an object, a commercial off-the-shelf controllable X/Y/Z table was used, see figure 4. Due to the foreseen amount of data to be analysed, it was decided to write the table control software in MatLab® too, just to have all system and data control in one software environment.

III. Signal Analysis

After completion of the hardware and writing the control software, data analysis had to be preformed. Initially, the data gathered was reduced in record length (10 ks), to minimize the

computational effort, but ultimately it is intended to use the entire memory record length and perform the analysis on it.

The main issue to be resolved is, how to synchronize the incoming periodic signals in such a way that an FFT can be performed with minimum amplitude, phase blur and leakage onto adjacent frequency spectral lines. For computational efficiency, the number of samples per interval should be equal to 2^N and in this ideal case no data filtering has to be applied, figure 5a. When asynchronous sampling is performed over a large non-integer number of signal periods, known Hamming or another type of filtering shall be used to prevent measurement interval discontinuities, figure 5b.

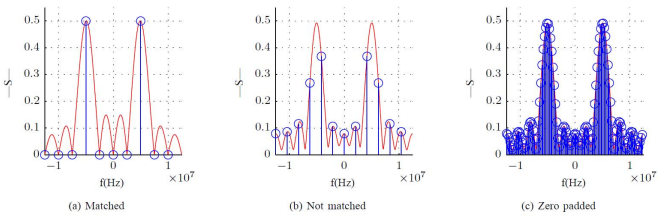

Figure 5 - Influence of FTT mapping on spectral plot

When the number of samples in the record length is nowhere near an integer multiple of the signal period, the measured frequency, amplitude and phase are affected. Several options occur: the record is extended by padding 'zeros' up to the next signal period or the record is extended with a large amount of zeros to increase the frequency resolution and to find a better estimate of the frequency, amplitude and phase. This results in the plot as shown in figure 5c. However, reduction of data can no longer be applied as all signal energy is spread out all over the frequency domain.

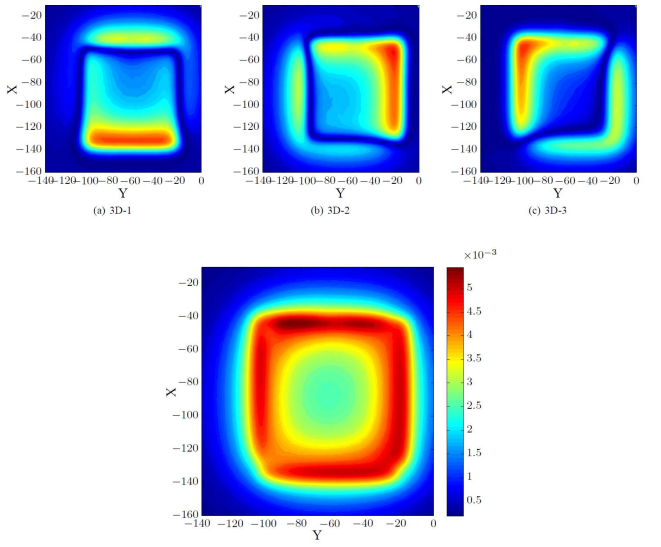

Figure 6 - H-field results obtained at 5 MHz, a/b/c/ are the individual readings from the orthogonal H-field rod antenna, the lower figure yields the composed result.

Another alternative is to synchronize and detect the signal's period exactly e.g. by using a Quadrature Signal Recovery Loop (QSRL) algorithm on the data obtained. Then the too low oversampled period can be interpolated: linear or cubic spline, such that 2^N samples apply over this fundamental period found. By doing so, both amplitude and phase are maintained spectrally. The latter case leads to the ideal case as depicted in figure 5a, amplitudes are correct; no spectral leakage occurs, phase information per spectral line remains stable and the spectral resolution/ accuracy has increased.

When the time-domain data is interpret correctly, and then only the related (sub-) harmonic signal amplitudes and their relative phases are needed to reconstruct the original signal with minimum error. As such the time-domain record length can be reduced down to two vectors which contain a few thousand harmonic amplitudes and phases. This means an effective data reduction ratio of 10^3 - 10^4.

Remember that a single surface scan, by taking a spatial resolution of 100 x 100 steps of an E/H-field in 3 orthogonal axis with 10 Ms/s/step/channel, results in $3 \cdot 10^{10}$ samples of raw data.

IV. Proof of Concept

The scanning method has been applied to a simple loop antenna, this to check the validity of the algorithms used. As can be seen in figure 6a/b/c, the individual H-field sensor amplitudes do not show the Cartesian H-field surface amplitudes one should expect. However, after correcting the data following the algorithm as described, the |H|-field plot, as given in figure 6, lower plot, results. Also a surface scan phase plot has been calculated and found to be in line with the expectations. The two: amplitudes and phases, can be combined in a vector plot (not shown).

The processed time domain data, even with limited record length (10 ks), does allow for deriving the first 10 harmonic H-field patterns from a single surface scan. These results shall be depicted in the presentation.

The RF front-end mixer system has been tested in the frequency range 2 – 20 GHz on all 4 channels simultaneously. The correction data obtained needs to be reduced and integrated in the signal flow.

This time-domain measurement concept can also be used for site surveillance or in-situ measurements. H-field measurements have been performed in the time-domain using a 0,25 m^2 shielded loop antenna. The 'real' H-field results e.g. expressed in A/m can be given in the time-domain again, then limited to the suitable bandwidth of 10 kHz to 30 MHz, being the bandwidth restrictions of the loop antenna used.

V. Conclusions

Carrying out RF emission surface or 3D scan measurements in the time-domain appears to be successful in

particular when multi-channel measurements can be taken in parallel such that orthogonal E/H-field data can be captured without any (re-) positioning alignment and synchronization issues.

Though the data sampling occurs asynchronous to the signals to be recorded, the exact fundamental period has to be derived e.g. by using the QSRL algorithm, this in combination with the synchronization signal obtained at the 4th scope channel. Doing so makes the time domain scanning method fast and extremely accurate and the post-processed data can be reduced by orders of magnitude without losing essential information.

The method by which the time-domain data is transferred into the frequency domain has a severe impact on the suitability of the data obtained. Fitting a periodic signal onto measurement period of 2^N samples to an integer multiple of the period of the signal appears to be the best solution to enable effective data reduction. In particular the use of zero padding delivers energy leakage over a broad frequency range which hinder the data reduction severely.

Due to the oversampling, limited by the record length i.e. memory depth of the oscilloscope used, the dynamic range of the measurement system can be enhanced by an order of magnitude or more compared to the vertical resolution of the oscilloscope itself.

To test for real EMC, no predetermined weighting filter and detector functions should be used as they block access to the detailed information required. The formal CISPR detectors and bandwidths apply for outdated broadcast systems and such measurement systems shall not be used for these kind of measurements. The spectral data obtained shall be integrated (vector sum over the bandwidth) according the target's sensitivities.

The calibration of E/H-field sensors, as carried out by commercial parties is debatable as large deviations were found between the probe correction data provided, measured and calculated. For this reason, a compact Helmholtz coil calibration system was build and tested.

The time-domain surface scan method has shown its feasibility but needs further enhancements, in particular in software. The time-domain measurement system could be build from off-the shelf components but needs to be extended further by E/H-field probes to cover the frequency ranges of interest. The sensitivity of the measurement system, when used with its full record length, becomes equal to or even superior to an RF spectrum analyzer performance.

The time-domain method provided can also be used to carry out site surveillance or in-situ measurements effectively. The integral field strength data gathered can be represented in the frequency or time domain. The latter is applied in: "Measurement methods for measuring voltages and electric fields as defined in the Dutch EMC Policy guide", NEN 2010.

FUTURE WORK

By using synchronization between the channels sampled, also program cycle synchronization to µC, DSP, FPGA can be performed, similar to the technique as described in IEC 62215-2: Integrated circuits - Measurement of impulse immunity - Part 2: Synchronous transient injection method, 2007.

Next to the RF emission scan method realized, also an RF immunity scan method will be developed to characterize the target's response to local E/H-fields applied.

ACKNOWLEDGMENT

The work has been carried out in close cooperation with ASML and the University of Technology in Eindhoven. The work carried out is supported by a Dutch Governmental innovation program WBSO, under number: ZT09051042.SO.

REFERENCES

[1] C.Hoffmann, P. Russer, A Real-Time Low-Noise Ultra-broadband Time-Domain EMI Measurement System up to 18 GHz, IEEE Transactions on Electromagnetic Compatibility, Nov 2011, pg. 882.
[2] Anton P. de Koning, Sensor Qualification Project, Dec 2011, TUE.
[3] Haitham Hassanieh, Piotr Indyk, Dina Katabi, Eric Price, Simple and Practical Algorithm for Sparse Fourier Transform, MIT, SODA, Jan. 2012, {haithamh,indyk,dk,ecprice}@mit.edu
[4] Detectus AB. EMC scanner products. http://www.detectus.se/products emc.html.
[5] Detectus AB. High resolution emc scanner. http://www.detectus.se/downloads/brochure-hr1-ic.pdf.
[6] Dusan Agrez. Improving phase estimation with leakage minimization. IEEE T. Instrumentation and Measurement, 54(4):1347–1353, 2005.
[7] Christian Reinhold et al. Presentation of a new 3d near-field scanner system for the analysis of emission and immunity in electronic systems. Presentation,2010. http://www.smart-systems-integration.org/public/documents/presentations/presentations-at-the-eposs-annual-forum-2010/annual-forum-8-october- 2010/session-3-design-manufacturing-and-interface-challenges/3-3-3D%20Nearfield%20Scanner%20System-Reinhold-Uni%20Paderporn-ENAS.pdf.
[8] Vladimir A Mandelshtam and Howard S Taylor. Harmonic inversion of time signals and its applications. The Journal of Chemical Physics, 107(17):6756, 1997.
[9] B. G. Quinn. Estimation of frequency, amplitude, and phase from the DFT of a time series. Signal Processing, IEEE Transactions on, 45(3):814–817, 1997.
[10] Tom´as Radil, Pedro M. Ramos, and A. Cruz Serra. New spectrum leakage correction algorithm for frequency estimation of power system signals. IEEE. Instrumentation and Measurement, 58(5):1670–1679, 2009.
[11] S. Schuster, S. Scheiblhofer, and A. Stelzer. The influence of windowing on bias and variance of dft-based frequency and phase estimation. Instrumentation and Measurement, IEEE Transactions on, 58(6):1975 –1990, june 2009.
[12] S.E. Schwarz. Electromagnetics for engineers. Saunders, 1995.
[13] WaveControl. Wavecontrol emxpert. http://www.wavecontrol-emc.com/en/57879/Producten-n2/EMC-Scanner-EMxpert.htm.